Infra-red organic light emitting devices

R.J. Curry. Optoelectronics Research Centre, University of Southampton, Southampton, SO17 1BJ, United Kingdom.

W.P. Gillin, Department of Physics, Queen Mary, University of London, Mile End, London, E1 4NS, United Kingdom.

ABSTRACT

We have demonstrated that it is possible to produce organic light emitting diodes (OLEDs) containing lanthanide ions which provide sharp electroluminescence emission at a range of wavelengths in the near infrared including 0.9 μm, 0.98 μm, 1.064 μm, 1.3 μm and 1.5 μm. For devices grown on ITO substrates we have demonstrated bright electroluminescence at drive voltages of ~12 V. We have shown that these diodes can be integrated onto silicon substrates and use the silicon as the anode of the device. For erbium based devices on silicon which emit at a wavelength of 1.5 μm we have demonstrated devices with room temperature internal efficiencies of approximately 0.01% at a drive voltage of 33 V.

1. INTRODUCTION

A technology which allowed for the efficient emission of light from a silicon based device would have a number of applications such as in telecommunications or for optical interconnects between integrated circuits. Such optical interconnects could theoretically provide very high data rates which would be immune from electromagnetic interference. Several methods have been used to try to get emission directly from silicon such as using Si:Ge superlattices to make pseudo-direct band gap devices [1], doping of silicon with erbium [2] which has an intra-atomic transition at 1.5 μm, and the use of ion implantation to produce layers of β-iron disilicide which is believed to be a direct band gap semiconductor [3]. Of these approaches the last two have been able to demonstrate 1.5 μm electroluminescence although neither has yet been able to produce a useful room temperature device. An alternative approach to obtaining optoelectronic devices on silicon substrates has been to grow relaxed buffer layers on to silicon substrates that allow the lattice constant to be sufficiently modified to grow direct band gap III-V devices on to the silicon [4]. Whilst this approach has shown some promise it is not clear whether the technology could be made compatible with silicon processing. More recent developments based on using the local strain field introduced by dislocation loops to keep carriers away from non-radiative centers in silicon have shown considerable promise for producing a ~ 1μm source [5]. However, there is still a need for a simple means of producing a silicon based 1.5μm source technology which operates at room temperature. The approach that we have been developing [6-10] is the integration of organic light emitting diodes which contain lanthanide ions directly onto a silicon substrate which acts as the anode for the devices. This approach allows us to make light emitting devices which operate at a range of wavelengths from the visible to the mid-infrared.

Organic light emitting diodes (OLEDs) have been the subject of a rapidly growing research activity since Tang and VanSlyke [11] demonstrated visible electroluminescence from a diode formed by the vacuum sublimation of two organic molecules on to an indium tin oxide (ITO) coated glass substrate in 1987. Research into these materials and devices have improved them to such an extent that devices emitting in the visible region have now been fabricated with external efficiencies of >15% [12] and projected lifetimes of 10^7 hours [13]. In order to improve the color saturation for visible OLEDs a number of groups started to incorporate lanthanide ions in to organic molecules. For example Kido *et al.* [14] incorporated europium which gives a narrow red emission line due to an intra-atomic transition within the 4*f* shell. The use of lanthanide containing compounds also has an additional advantage. Spin statistics limit the theoretical internal efficiency of conventional OLEDs to 25% as only singlet excitons can combine radiatively [15]. For the lanthanide containing molecules however, triplet excitons, which comprise 75% of the available excitons in an OLED, can couple to the lanthanide ions transferring their energy and thus potentially improving device performance [16]. Furthermore, the presence of the lanthanide ion increases the spin-orbit coupling and hence the probability of intersystem crossing between singlet and triplet excitons in these devices.

The use of organolanthanides for infrared sources is attracting increasing interest and devices containing erbium for 1.5 μm emission, neodymium for 0.9 μm, 1 μm and 1.3 μm emission and ytterbium for 0.98 μm emission have now been demonstrated [7,8,10,17-20]. All of these devices have so far relied on the use of indium tin oxide (ITO) coated glass substrates as used for the visible light emitting devices, however, we have shown that it is possible to deposit an erbium

based OLED directly on to a silicon substrate to produce a room temperature 1.5 μm emitting device [9]. Due to the relatively simple vacuum sublimation process needed to produce these devices we believe that this technology should be suitable for producing silicon based integrated optoelectronic devices. Indeed recent work by Mathine *et al* [21] has demonstrated the integration of an array of visible surface-emitting OLEDs directly on to a CMOS circuit. As has been demonstrated for visible OLEDs, organic devices now have sufficient lifetimes for them to find applications even in telecommunications systems.
In this paper we present a review our initial 'proof of concept' devices and highlight a number of issues that need to be addressed in order to improve device efficiency towards that required for second generation devices.

2. EXPERIMENTAL METHOD

Each of the lanthanide *tris*(8-hydroxyquinoline) (LnQ) molecules were synthesised as previously reported [7,8,10] and are shown in figure 1. Prior to sublimation to form OLEDs the materials were heated to 150°C in a vacuum (~10^{-6} mbar) to remove any volatile impurities and water that may be present from the synthesis. Analysis of sublimed films of the synthesised ErQ was carried out using Rutherford backscattering and the atomic ratios obtained were within 1% of the theoretical ratios for this molecule [22].
OLEDs were fabricated by vacuum sublimation on to either (100) boron doped CZ silicon with a resistivity of 0.01-0.02 Ω.cm or on to indium tin oxide (ITO) coated glass substrates with a sheet resistivity of 20 Ω/□. For the devices grown on silicon substrates the wafer was cut in to 20 mm x 20 mm squares and prior to the organic deposition the substrates were patterned with a 50 nm thick layer of plasma enhanced chemical vapor deposited (PECVD) silicon nitride. This was deposited to provide isolation regions to prevent the top contact from shorting to the underlying silicon substrate when electrical contact was made to the devices. No attempt was made to remove any native oxide that may have been present on the silicon surface prior to the organic evaporation. To provide electrical contact to the silicon substrate a 20 nm layer of aluminum was evaporated, no sintering of this contact was used.
For the OLEDs deposited on to ITO substrates the ITO was cut in to 20 mm x 20 mm squares, as for the silicon substrates. The ITO was then patterned to give a central region that provided the anode contact and bare glass regions to the sides where the cathode material was subsequently evaporated. Prior to the organic deposition the substrates were cleaned, in an ultrasonic bath, using an organic solvent process consisting of dichloromethane, acetone and methanol. Some of these substrates were then further cleaned and oxidized using treated in an O_2 plasma treatment.
On both substrates the same diode structures were grown, figure 1. The OLEDS were fabricated using a 40 nm layer of N,N'-diphenyl-N,N'-bis(3-methylphenyl)-1,1'-biphenyl-3,3'-diamine (TPD), figure 1, as the hole transport layer, which was deposited directly on to the substrate at a rate of 1-2 Å/s. To obtain this evaporation rate a source temperature of ~220°C was used. Following this a 50 nm layer of one of the lanthanide tris(8-hydroxyquinolines) (LnQ) was deposited, at a rate of 2-3 Å/s, which acted as both an electron transporting layer and the emitting layer. The source temperature for the LnQ evaporation was ~410°C. Finally a 200 nm layer of aluminum was deposited as the cathode contact. All the film thicknesses were measured using a quartz crystal monitor. The base pressure in the evaporation chamber was ~10^{-7} mbar and during evaporations the pressure was ~10^{-6} mbar.

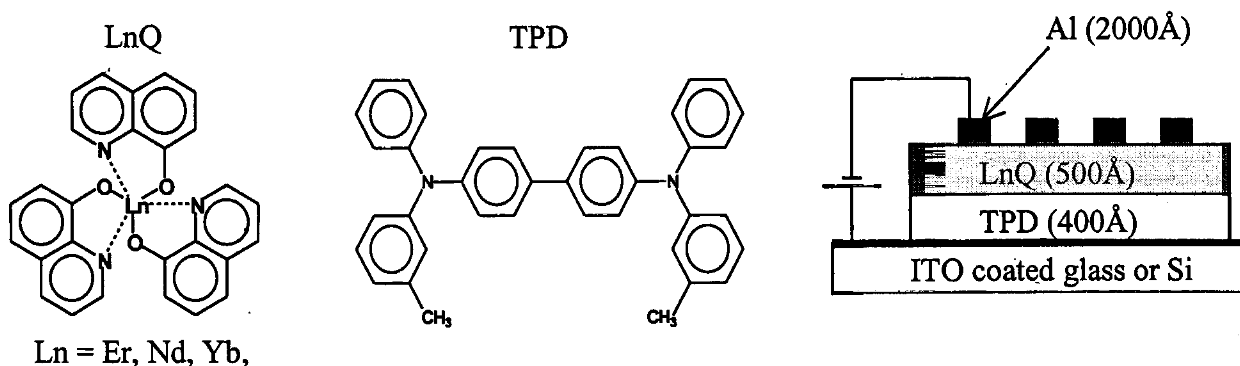

Figure 1. Molecules used to fabricate infra-red emitting OLEDs and a schematic of an OLED device structure.

For the silicon based diodes only ErQ was used as silicon is transparent at the emission wavelength for the $^4I_{13/2}$ to $^4I_{15/2}$ transition in Er^{3+} at 1.5 μm. The electroluminescence from the diode was recorded at room temperature and collected

through the back surface of the silicon. This back surface was the chemically etched surface of the as received wafer. No extra roughening of this surface, which may improve the external efficiency, was performed. All the lanthanide containing molecules were used to produce diodes on the ITO substrates. Again the luminescence from these devices were recorded through the back surface. All measurements were obtained with the devices operating in air. The infrared luminescence was dispersed in a 1 meter scanning spectrometer fitted with a 1 μm Blazed grating and detected using a liquid nitrogen cooled germanium p-i-n diode. For the visible region a 0.5 μm Blazed grating was used to disperse the luminescence and it was detected using an S-20 photomultiplier tube. Standard lock-in detection techniques were used for the collecting the luminescence and frequency resolved spectra. Current – voltage (I-V) measurements were performed using a Keithley 236 source – measure unit.

3. RESULTS

3.1 Erbium *tris*(8-hydroxquinoline) based OLEDs

Figure 2 shows the visible electroluminescence spectra for an ITO based ErQ OLED at 300 K and 100 K. The broad emission peaking at ~ 520 nm is due to the recombination of excitons on the ligands of the molecule. The sharper emission peaks seen superimposed onto this ligand luminescence at ~402 nm, ~ 430 nm, and ~ 650nm originate from intra-atomic transitions from the $^2H_{9/2}$, $^4F_{3/2}$, and $^4F_{9/2}$ to the $^4I_{15/2}$level in the Er^{3+} ion [23]. Figure 3 gives a schematic of the Er^{3+} energy levels along with the wavelengths of various transitions. The peak seen at ~ 800 nm in the 300 K spectra is the second order 400 nm peaks. Emission from these high energy transitions is also observed in the photoluminescence spectra obtained using an excitation wavelength of 363 nm and 351 nm. However, when an excitation wavelength of 457 nm or above is used only the ligand luminescence is observed even at high pumping densities (upto 500 mW) [22].

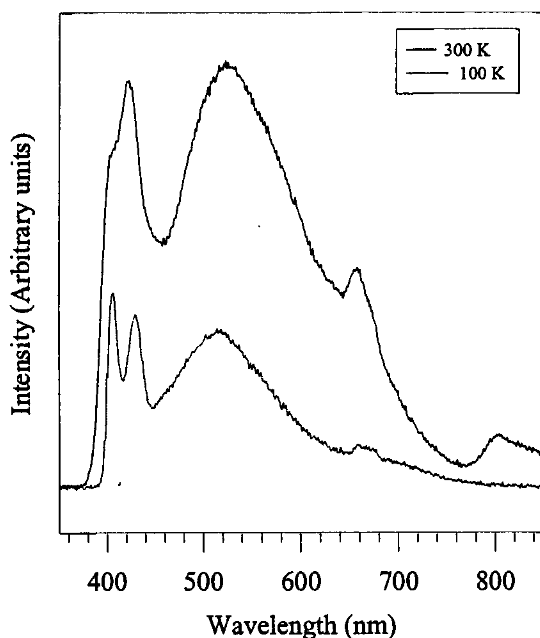

Figure 2. The electroluminescence spectra of an ErQ based OLED fabricated on ITO coated glass. Driving voltage = 30V

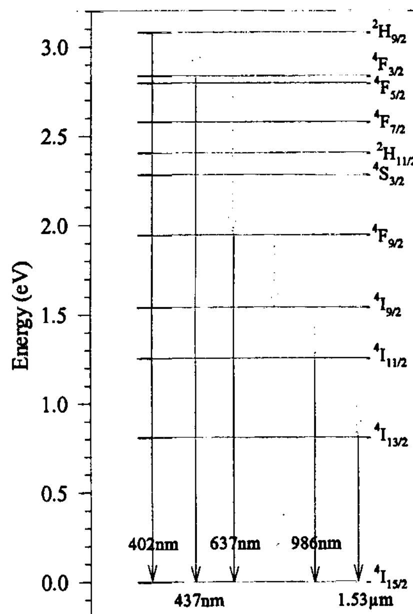

Figure 3. Schematic of the intra-atomic energy levels in the Er^{3+} ion [23].

This indicates that to obtain emission from these levels requires the direct excitation of an electron from the $^4I_{15/2}$ level to a high energy level (i.e. $^2H_{9/2}$ or above) and that such excitation does not take place through an upconversion process within the Er^{3+} ion. The high energy of the transition would require the transfer of energy from a singlet exciton on the ligand into the Er^{3+} ion. The Förster transfer (dipole-dipole coupling) of singlet excitons to the Er^{3+} ion is possible and has been

observed in Eu^{3+} containing molecules [14]. It should be noted that in recent devices [7] such high energy emission from the Er^{3+} ion has not been present in the visible electroluminescence spectra and the ligand emission is seen to peak at ~ 600 nm [22]. The reason for this change is under investigation but it may be related to the synthesis and purification of the molecules used in each case. Another possibility may be that the higher voltages used to drive the early devices, in which the ITO was not treated with an O_2 plasma, enabled direct excitation of the Er^{3+} ion through hot electron impactation.

Figure 4 shows the electroluminescence spectra of an ErQ based (ITO) OLED from the visible to the near infrared. It can be seen that the spectra consists of a number of sharp emission lines with the prominent emissions occurring at ~1.5 µm, 0.98 µm and a broad emission in the visible region. The 1.5 µm emission is due to the transition between the $^4I_{13/2}$ and $^4I_{15/2}$ levels and is the strongest emission line present, figure 3. It is this emission line which is the basis for erbium doped fiber amplifiers (EDFA) and is the key wavelength for long distance telecommunications systems [24]. The weaker line at 0.98 µm is due to transitions between the $^4I_{11/2}$ and $^4I_{15/2}$ levels. It is absorption into this level which is the main means for the optical pumping of EDFAs. The broad visible emission partly consists of emission from triplet excitons on the organic ligands and partly due to some higher energy transitions within the erbium ions such as from the $^2H_{9/2}$, $^4F_{9/2}$, $^2H_{11/2}$ and $^4S_{3/2}$ levels.

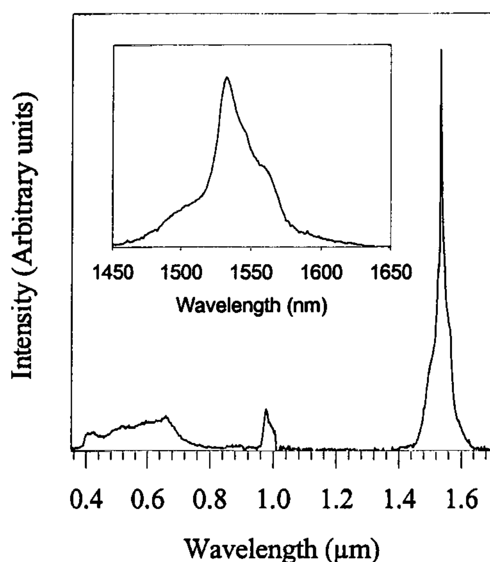

Figure 4. The electroluminescence spectra of an ErQ (ITO) based OLED driven at 25V.

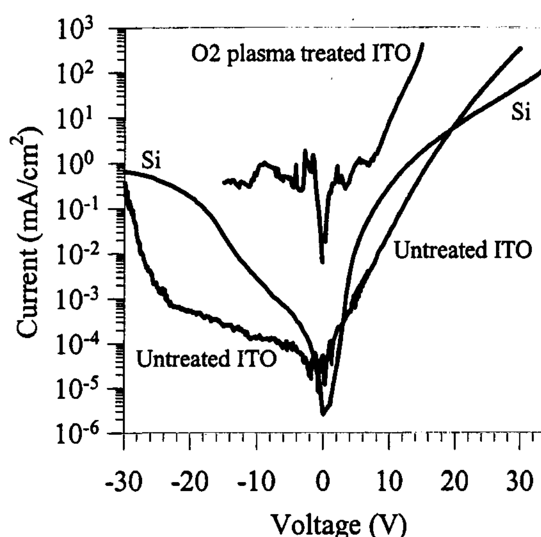

Figure 5. The I-V characteristics of an ErQ based OLED. Note that the y-axis shows absolute current density.

In these devices the ligand luminescence has shifted to a lower energy to that seen in our early devices. This emission at ~ 600 nm originates from the recombination of triplet excitons. The fact that triplet luminescence is visible form these devices is interesting. Normally in OLEDs it is possible to observe bright singlet emission but the radiative recombination of the triplets is spin forbidden. However, in these devices we observe no or very little singlet emission and this suggests that the singlet excitons may be coupling very efficiently to the erbium ions, as is implied in figure 2. An alternative explanation for the lack of singlet emission in this spectrum could be that a structural deformation of the molecule due to the large size of the erbium ion may give an alternative non-radiative route for recombination. Further work will be necessary to understand this observation fully. Although triplet emission is normally spin forbidden the large mass of the erbium ion enhances spin-orbit coupling and increases the probability of radiative triplet recombination (phosphorescence).

These ITO based diodes show good diode-like I-V characteristics with the diodes starting to break down in reverse bias at ~-24 V, see figure 5. In forward bias the current voltage behavior is consistent with trap limited conduction as proposed by Burrows *et al.* [25] for charge transport in AlQ based devices. Our original devices, shown in figure 4, have turn on voltages of ~15 V and demonstrate useful electroluminescence at drive voltages of ~25 V which corresponded to current densities through the diodes of ~50 mA/cm². Our more recent ITO based devices which have had the ITO substrates treated in an O_2

plasma for 60 seconds have turn on voltages of ~7V and support current densities of >500 mA/cm^2 at drive voltages of ~12V.

Due to the fact that silicon is transparent at 1.5 μm, ErQ is an ideal material for investigating the incorporation of infrared OLEDs directly on to silicon substrates. Figure 5 also shows the I-V characteristic for an OLED with the same layer thicknesses as that grown on ITO but which uses the p^{++} silicon substrate as the anode contact. It can be seen that for this diode the initial turn on of the diode is much sharper, with a four order of magnitude increase in current between 0 and 6 V. However, for higher voltages the rate of increase in the current slows dramatically, this may be a reflection of poor hole injection from the silicon anode, but more work will be needed to understand this behavior properly. For these silicon based diodes we have made no attempt to optimize the organic/silicon interface for charge injection.

Figure 6 shows the electroluminescence spectra from the $^4I_{13/2}$ and $^4I_{15/2}$ level for the silicon based device recorded at a drive voltage of 33 V. Due to the high absorption coefficient of silicon at wavelengths below 1.1 μm none of the other transitions visible in the ITO based diodes can be seen in the silicon based devices. The inset to figure 5 shows the intensity of this 1.5 μm emission as a function of the current density through the device. From this inset it can be seen that the intensity has a sub-linear dependence on the current density. We do not know the reason for this sub-linear behavior but we do not believe that it is related to the long lifetime for the erbium transition resulting in saturation. For erbium implanted silicon devices it has been shown that this long lifetime coupled with the relatively low concentration of erbium ions that could be introduced would result in emission intensities that would be too small to be useful as conventional LEDs [26]. For our organic devices we have measured the recombination lifetime to be of the order of ~200 μs [22] and given that we have ~10^{14} erbium ions in our devices, for a device area of 4 mm^2, we estimate that our devices would have a theoretical maximum internal optical power generation of ~100 mW. This would be more than enough for a useful LED. Naturally if the devices were to be incorporated in to laser structures this limitation imposed by the spontaneous lifetime would cease to apply and even higher power outputs should be possible. We have estimated the internal efficiency for our silicon devices to be ~0.01% at the operating voltage of 33 V. Although this value is very low we believe that it should be possible to greatly improve this value through improvements to device design and processing.

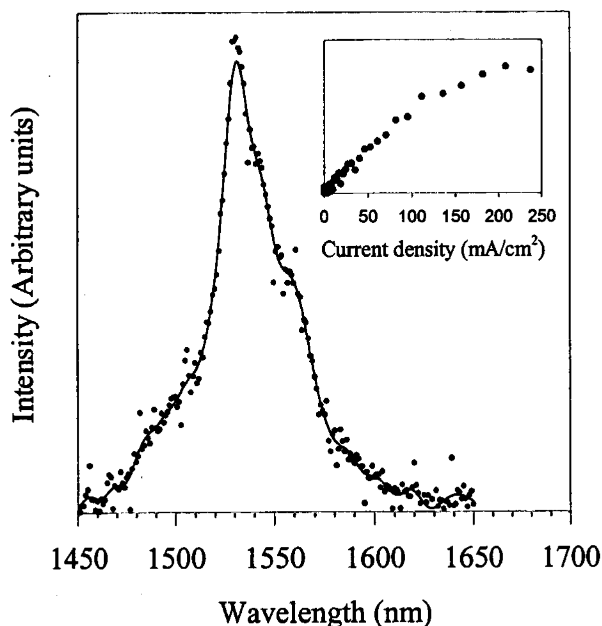

Figure 6. The electroluminescence spectra from a TPD/ErQ diode grown on a silicon substrate driven at 33 V. The inset shows the intensity of this emission, at 1.532 μm with a resolution of ~4 nm, as a function of the current density through the device.

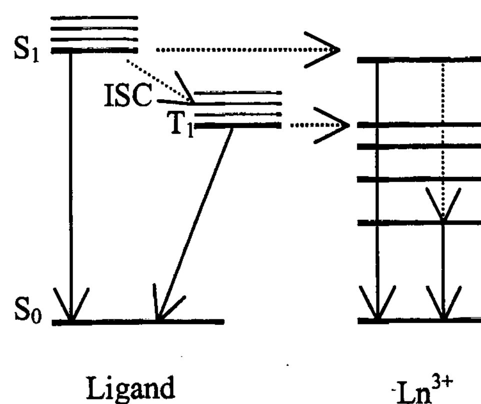

Figure 7. The proposed energy transfer mechanism from the ligand to lanthanide ion in LnQ. Solid and dashed lines represent radiative and non-radiative transitions respectively. ISC = intersystem crossing, S and T represent singlet and triplet states respectively.

Figure 7 shows a schematic diagram of the proposed energy transfer mechanism in LnQ. In this proposed mechanism singlet excitons transfer energy to the Ln^{3+} ion through a Förster process as previously discussed. Due to the short radiative lifetime of singlet excitons it would generally be expected that this process is not very efficient. Energy transfer from the

ligand to the Ln^{3+} ion in such a case is expected to be dominated by the transfer of energy from triplet excitons to the ion. However, in these molecules the large ion increases the spin-orbit coupling and so intersystem crossing between the singlet and triplet states becomes a significant process. This then should allow a large proportion of the created excitons to transfer their energy into the Ln^{3+} ion thus improving the device efficiency. Once energy has been transferred into the Ln^{3+} ion the excited electron will relax to a metastable level through a non-radiative process. In these molecules the high phonon energy is ~0.2 eV [27] so rapid relaxation occurs between intra-atomic energy levels separated by this energy, figures 3 and 8. Once the excited electron has relaxed to a metastable level emission can then occur through a forced electic dipole transition. In reference [28] a review of the selection rules for intra-atomic transitions is given. Further work on the morphology, Stark splitting and thermal stability of ErQ is in preparation for publication[29].

3.2 Neodymium *tris*(8-hydroxquinoline) based OLEDs

Neodymium has a bright emission line at ~1.064 μm which is due to transitions between the $^4F_{3/2}$ and $^4I_{11/2}$ levels, figure 8 and 9. It is this transition which is responsible for the high power 1 μm Nd:YAG laser output. In addition to this transition there are also two other near infrared emission lines that can be obtained from neodymium; one at ~900 nm which is due to the $^4F_{3/2}$ to $^4I_{9/2}$ transition and one at ~1.3 μm which is due to the $^4F_{3/2}$ to $^4I_{13/2}$ transition. The 1.3 μm transition has been extensively studied with regard to producing a fibre laser and amplifier at this wavelength as this is the low dispersion window in silica [30]. We have fabricated NdQ diodes on to ITO substrates and the electroluminescence spectra from one of these diodes is shown in figure 9. It can be seen that the diodes exhibit bright electroluminescence at 1.064 μm as well as luminescence from the other two infrared transitions at ~900 nm and 1.3 μm. The 1.3 μm luminescence from this diode is only about 10% of the intensity of the main 1.064 μm luminescence however, for a silicon based device this transition would be below the band gap of the silicon and hence the silicon would be transparent. This transition from a NdQ based device could therefore be potentially used for a silicon based OLED. The I-V characteristics are similar to that shown in figure 5 for ErQ diodes and so is not shown [8].

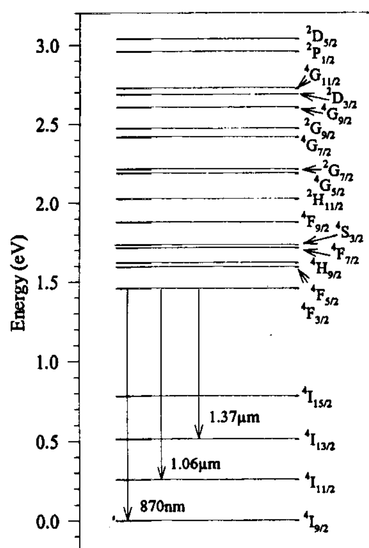

Figure 8. Schematic of the intra-atomic energy levels in the Nd^{3+} ion [23].

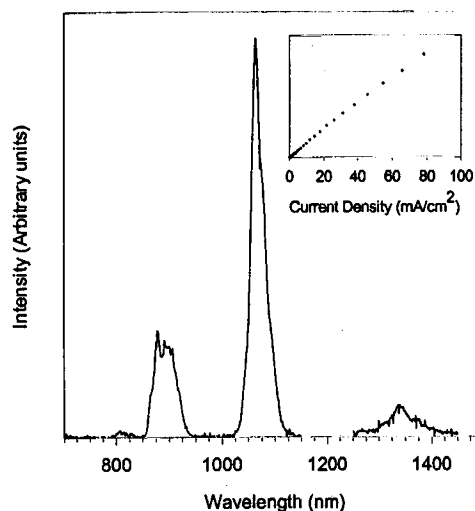

Figure 9. The electroluminescence spectra from a NdQ based diode grown on to an ITO substrate driven at 30 V. The inset shows the intensity of the 1064 nm emission, in arbitrary units, as a function of the current density through the device.

The inset to figure 9 shows the intensity of the 1064 nm emission with driving current. Again there is a slight sub-linearity with increasing current density and further work is needed to investigate the origin of this behaviour. The energy transfer mechanism in NdQ is the same as for ErQ. A comparison of the intra-atomic energy levels of Er^{3+} and Nd^{3+}, figures 3 and 8, shows that the higher levels are much closer packed in energy in the case of the Nd^{3+} ion. Any transfer of energy exciting an

electron above the $^4F_{3/2}$ level in this case would result in rapid non-radiative relaxation to the $^4F_{3/2}$ level. From this level radiative recombination occurs through a forced electric dipole transition.

3.3 Ytterbium *tris*(8-hydroxquinoline) based OLEDs

Ytterbium is unusual amongst the lanthanides in that the 4*f* shell for Yb^{3+} is only one electron short of being filled. As a consequence the entire energy level scheme consists of only an inverted ^2F level [23]. This gives a single set of Stark split emission lines at around 980 nm ($^2F_{5/2}$ level). The ligand luminescence of YbQ is very similar to that of the other molecules presented here peaking at ~ 600 nm (~ 2.06 eV). From this we infer that the energy of the excitons formed on the ligands is in the range ~2 eV to 2.4 eV [10] for triplet and singlets respectively. The $^2F_{5/2}$ and $^2F_{7/2}$ levels in Yb^{3+} have an energy separation of ~ 1.27 eV and so there is a large mismatch between the lowest energy of the excitons formed on the ligands and this intra-atomic transition. If the energy transfer process in YbQ were the same as for ErQ and NdQ then one would expect to see no emission from the Yb^{3+} ion as energy transfer into the ion is not possible.
However, this energy difference does not appear to be an obstacle to energy transfer as the electroluminescence spectra for an ITO based diode containing YbQ shows, figure 10. Such transfer has also been noted in other similar systems containing Yb^{3+} [31-34].

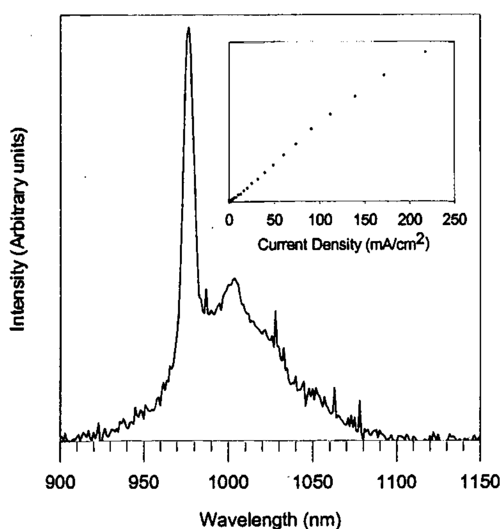

Figure 10. The infra-red electroluminescence obtained from a YbQ based (ITO) OLED operating at 25V. The inset shows the intensity of this emission as a function of current density.

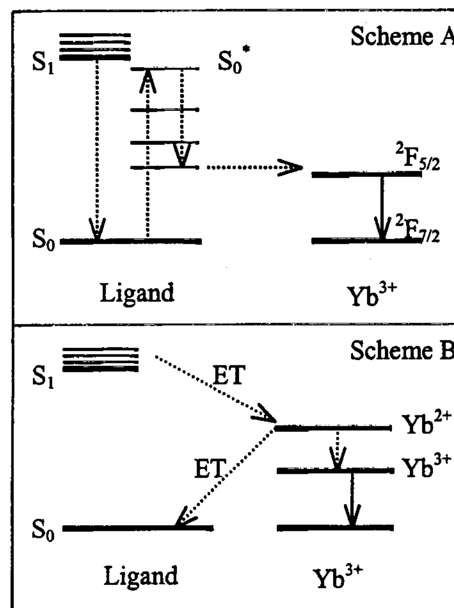

Figure 11. Two possible schemes for the transfer of energy from the ligand into the Yb^{3+} ion. S_0= singlet ground state, S_1 = 1st electronic excited singlet state. S_n^*= vibration state of electronic level n. ET= electron transfer.

This electroluminescence spectra shows a clear narrow emission peak at 980 nm in addition to some weaker features at lower energies. For all the lanthanide ions the emission spectra splits in to a number of Stark levels due to the local electric field experienced by the ion and it is this Stark splitting which is responsible for the low energy features, at around 1 μm, found in figure 10. The I-V characteristic for the YbQ diodes are very similar to those for the ErQ diodes and hence we have not shown them [10]. The inset to figure 10 shows the intensity of the emission as a function of the current density in the device.
Given that the energy transfer mechanism in ErQ and NdQ cannot be applied for YbQ a new mechanism must be found to explain this emission from the Yb^{3+} ion. Figure 11 shows two proposed mechanisms by which energy transfer into the Yb^{3+} ion could occur. In scheme A, the mechanism proposed by Crosby *et al.* [31], coupling occurs between the excited singlet

state (S_1) and high vibrational states of the ligand (S0*). Vibrational levels of ligand can then couple with $^2F_{5/2}$ Yb^{3+} level. Emission is then observed from the $^2F_{5/2}$ to $^2F_{7/2}$ intra-atomic transition. In scheme B, proposed by Kirk *et al.* [35], electron transfer takes place from the ligand to the Yb^{3+} ion creating a radical cation and Yb^{2+}. Due to the fact the the former of these is a strong oxidant and the later a strong reducing agent the electron is returned to the ligand. As the energy of the Yb^{2+} system is greater than that of the $^2F_{5/2}$ level in the Yb^{3+} ion an excited state of this ion can be produced. Emission is then observed from the $^2F_{5/7}$ to $^2F_{7/2}$ intra-atomic transition. Further work is necessary before the process of energy transfer is understood in Yb^{3+} containing chelates though from our results it appears that the transfer of energy into the ion is not a temperature dependant process [10].
The emission wavelength of 980 nm obtained from the YbQ diodes is the key pump wavelength for EDFAs and this would be a key application for these devices. However, as the emission wavelength is above the band gap for silicon these devices could also have applications for inter-chip communications. Naturally because the 980 nm emission is strongly absorbed by silicon we could not make devices on silicon with YbQ using the same technology as we used for the ErQ devices, i.e. with emission through the back surface. However, there have been reports in the literature of using n-type silicon as an electron injecting contact into visible OLEDs, and the use of an ITO anode as a transparent top contact is well reported [36]. Using this approach it should be possible to fabricate surface emitting 980 nm LEDs on to silicon substrates.

4. DISCUSSION

4.1 Device structure

In order to try and improve the performance of these devices there are a number of changes that could be made to improve the charge injection and transport in the devices. Current diode structures are much more advanced than the ones used here for our proof of concept devices [37]. Future devices will need to make use of these more efficient structures if high efficiencies are to be realized. For example, the aluminum cathodes that we have used are known to be relatively poor electron injectors in AlQ devices and that using low work function metals for the cathodes can significantly improve the electron injection [38]. For the anode contact there has been very little work on improving the silicon/organic interface for hole injection unlike the ITO/organic interfaces. However, in order to improve the hole injection there are several approaches that could be used, such as removing any native oxide prior to organic deposition, using ion implantation to change the doping concentration in the silicon surface, introducing a thin ITO hole injector on to the silicon surface or changing the organic hole transport layer. All of these approaches will require significant research effort to produce the optimum anode system. However, it should be noted that Mathine *et al* [21] has demonstrated that it is possible to integrate an array of conventional visible emitting OLEDs directly on to a complementary metal-oxide-semiconductor (CMOS) circuit. These devices were operated with a compliance voltage of ~10 V although they state that they have improved their process so that they can achieve turn on voltages on silicon based devices of 2.5 V. This is very encouraging for the possibility of integrating our devices in to a silicon based optoelectronic device.
A more advanced structure would also allow us to remove the need for the lanthanide containing molecule to function as the electron transporting layer in the device. This would allow the investigation of a new range of lanthanide containing molecules who's main function would be as an emitting material. Finally, in such devices codoping the emitting layer with both Yb^{3+} and Er^{3+} containing molecules may offer an additional route to increasing the emission yield from the Er^{3+} ion.

4.2 Molecular design

We have shown that it is possible to obtain electroluminescence at a number of wavelengths in the infrared using different rare earth ions incorporated in to organic molecules. In order to improve the efficiency of the devices it is essential to fully understand the mechanism of energy transfer from the ligands to the rare earth ion. Once this is understood it may be possible to synthesise new molecules tailored to the rare earth ion incorporated. If energy transfer occurs predominantly through the coupling of triplet excitons in a Dexter type process then it is essential to minimise the distance between the ligands and the rare earth ion [39].
One major source of luminescence quenching in rare earth containing materials is due to energy transfer from the ion to OH^- groups. It is therefore essential to avoid incorporating such groups into these molecules if high luminescence efficiency is required. Similarly the high phonon energies of many materials reduce the emission cross section for many intra-atomic transitions. As such it may be advantageous to synthesise fluorinated molecules as this should reduce the high phonon energy and may increase the emission cross section of some intra-atomic transitions. Such fluorination may also effect the vapor pressure of the molecules which is an important parameter when producing vacuum sublimed films.

The environment that the rare earth containing molecule creates around the ion is responsible for the Stark splitting of the intra-atomic energy levels. This Stark splitting defines what the shape of the emission spectra of each transition will be. For applications where wavelength division multiplexing (WDM) is to be used it is advantageous to have broad emission. As a consequence it may be possible to design molecules with high or low symmetry around the rare earth ion to decrease or increase the full width at half maximum (FWHM) of the emission respectively. For the $^4I_{13/2}$ to $^4I_{15/2}$ transition seen in ErQ based devices the FWHM is ~ 80 nm.

4.3 Future device applications

The OLED devices produced from these molecules can be integrated on to silicon substrates with the silicon acting as the anode for the device. Currently we have focused on erbium due to its potential for the telecommunications industry, however, for applications such as optical interconnects the 1.5 μm wavelength produced by erbium may not be the ideal choice. This would mainly be due to the difficulty in integrating a detector that operates at this wavelength on to silicon substrates. This is not an insurmountable problem as there are already technologies being developed such as relaxed buffer layers [4] which may allow germanium photodiodes to be grown directly on to silicon or alternatively β-iron disilicide [3] which can be formed on silicon may also have a use as a detector.

If an optical interconnect technology that relied on silicon photodiodes was required then we have shown that ions such as ytterbium and neodymium can be used to produce emission at wavelengths around 1 μm. With these materials devices would need to be made which were surface emitters. However, the technology to produce visible light emitting OLEDs on silicon substrates has already been demonstrated and this technology is immediately applicable to this class of infrared OLEDs.

One potential drawback to the use of infrared OLEDs for communications would be their speed of operation. For many of the rare-earth ions the spontaneous lifetimes are relatively slow, in addition with the low mobilities of the organic molecules and the potentially long lifetime of excitons, particularly triplets, this may seriously affect their use in a number of applications. However, there are ways that even these potential problems may be overcome. For the longer wavelength emissions such as the erbium $^4I_{13/2}$ to $^4I_{15/2}$ transition at 1.5 μm or the neodymium $^4F_{3/2}$ and $^4I_{13/2}$ transition at 1.3 μm where the silicon is transparent it may be possible to integrate the OLED in to a silicon waveguide cavity and operate the device as a CW laser. High speed modulation could then in theory be provided through the use of a modulator either internal or external to the cavity.

We have found that because the emission wavelength is determined by an intra-atomic transition within the ion, which is very effectively shielded from external perturbations, there was no temperature dependence of the emission wavelength at temperatures down to 4 K. However, the electrical performance of the diodes does depend on the operating temperature with the drive voltages required to obtain luminescence increasing as the temperature is reduced. However, we have been able to demonstrate ErQ devices on ITO substrates operating at 100 K.

The organic molecules used in these devices are all deposited from relatively low temperature sources and do not need any thermal processing following deposition. Although we do not expect the layers to be able to cope with a typical CMOS device processing regime we believe that the deposition of the OLED, which consists of a number of evaporation steps should be possible as a final process in the fabrication of a device and as such should be compatible with the production of silicon integrated optoelectronic devices.

5. CONCLUSIONS

We have demonstrated that it is possible to obtain electroluminescence at a range of wavelengths in the infrared using lanthanide ion containing OLEDs. We have also demonstrated that it is possible to integrate these devices directly on to silicon substrates to produce devices which operate at room temperature. These initial devices have very high operating voltages although we believe that they can be greatly reduced with some alterations to the device processing. It should be noted that current state-of-the-art visible OLEDs have operating voltages of the order of 5 V. The device efficiency of our present devices is also very low, we estimate internal efficiencies of ~0.01%. Again we feel that this can be improved dramatically with improved device design and processing. Visible OLEDs have been reported which are operating with external efficiencies of ~15%.

6. REFERENCES

1. S.S. Iyer and Y.H. Xie. Science, **260**, 40-46 (1993).
2. A. Polman. J. Appl. Phys., **82**, 1 (1997).
3. D. Leong, M. Harry, K.J. Reeson and K.P. Homewood. Nature, **387**, 686 (1997).
4. S.F. Fang, K. Adomi, S.Lyer, H. Morkoc, H. Zabel, C. Choi and N. Otsuka. J. Appl. Phys., **62**, R31 (1990).
5. Ng. Lek, M.A. Lourenco, R.M. Gwilliam, S. Ledain, G. Shao and K.P. Homewood. Nature, **410**, 192 (2001).
6. W.P. Gillin and R.J. Curry. Appl. Phys. Lett., **74** (6), 798 (1999).
7. R.J. Curry and W.P. Gillin. Appl. Phys. Lett., **75** (10), 1380 (1999).
8. O.M. Khreis, R.J. Curry, M. Somerton and W.P. Gillin. J. Appl. Phys., **88** (2), 777 (2000).
9. R.J. Curry, W.P. Gillin, A.P. Knights and R. Gwilliam, App. Phys. Lett., **77** (15), 2271 (2000).
10. O.M. Khreis, R.J. Curry, M. Somerton and W. P. Gillin. Organic Electronics, in press.
11. C.W. Tang and S.A. Vanslyke. Appl. Phys. Lett., **51**, 913, (1987).
12. C. Adachi, M.A. Baldo, S.R. Forrest and M.E. Thompson. Appl. Phys. Lett., **78** 1704 (2000).
13. P.E. Burrows, S.R. Forrest, T.X. Zhou and L. Michalski. Appl. Phys. Lett., **76** (18), 2493 (2000).
14. J. Kido, H. Hayase, K. Hongawa, K. Nagai and K. Okuyama. Appl. Phys. Lett., **65** (17), 2124 (1994).
15. M.A. Baldo, D.F. O'Brien, M.E. Thompson and S.R. Forrest. Phys. Rev. B., **60**, 14422 (1999).
16. M.A. Baldo, M.E. Thompson and S.R. Forrest. Pure Appl. Chem.., **71** (11), 2095 (1999).
17. M. Iwamuro, T. Adachi,Y. Wada, T. Kitamura, and S. Yanagida, Chem. Lett., **7**, 539, (1999).
18. R.G. Sun, Y.Z. Wang, Q.B. Zheng, H.J. Zhang and A.J. Epstein, J. Appl. Phys., **87**(10), 7589, (2000).
19. Y. Kawamura, Y. Wada, M. Iwamuro, T. Kitamura and S. Yanagida, Chem. Lett., **3**, 280, (2000).
20. Y. Kawamura, Y. Wada and S. Yanagida, Jpn. J. Appl. Phys. 1, **40**(1), 350, (2001).
21. D. L. Mathine, H.S. Woo, W. He, T.W. Kim, B. Kippelen and N. Peyghambarian, Appl. Phys. Lett., **76**(26), 3849, (2000).
22. R.J. Curry. 'Luminescence characterization of aluminium and erbium *tris*(8-hydroxyquinoline)'. Thesis, University of London (1999).
23. G.H. Dieke, 'Spectra and Energy Levels of Rare Earth Ions in Crystals', John Wiley and Sons, New York, 1968.
24. E. Desurvire, 'Erbium-Doped Firbe Amplifiers', John Wiley and Sons, New York, 1994.
25. P.E. Burrows, Z. Shen, V. Bulovic, D.M. McCarty, S.R. Forrest, J.A. Cronin and M.E. Thompson. J. Appl. Phys., **79** (10), 7991 (1996).
26. Y.H. Xie, E.A. Fitzgerald and Y.J. Mii. J. Appl. Phys., **70** (6), 3223 (1991).
27. R.J. Curry, W.P. Gillin, J. Clarkson and D.N. Batcheldor, Submitted to J. Appl. Phys.
28. R.D. Peacock, 'Structure and Bonding 22: The intensities of Lanthanide *f-f* Transitions', Springer-Verlag, New York, 1975.
29. R.J. Curry, W.P. Gillin, J. Clarkson and D.N. Batcheldor, In preparation.
30. D. Hewak, 'Properties, Processing and Applications of Glass and Rare Earth-Doped Glasses for Optical Fibres', INSPEC, London, 1998.
31. G.A. Crosby and M. Kasha, Spectrochim. Acta, **10**, 377 (1958).
32. A. Abusaleh and C.F. Meares, Photochem. Photobiol., **39** (6), 763 (1984).
33. W.D. Horrocks, J.P. Bolender, W.D. Smith and R.M. Supkowski, J. Am. Chem. Soc., **119**, 5972 (1997).
34. Y. Kawamura, Y. Wada, M. Iwamuro, T. Kitamura and S. Yanagida, Chem. Lett., **3**, 280 (2000).
35. W.R. Kirk, W.S. Wessels and F.G. Prenderdast, J. Phys. Chem., **97**, 10326 (1993).
36. P.E. Burrows, G. Gu, S.R. Forrest, E.P. Vicenzi, T.X. Zhou, J. Appl. Phys., **87**(6), 3080 (2000).
37. S. Lamansky, P. Djurovich, D. Murphy, F. Abdel-Razzaq, H. Lee, C. Adachi, P.E. Burrows, S.R. Forrest and M.E. Thompson, J. Am. Chem. Soc., **123**, 4304 (2001).
38. L.S. Hung, C.W. Tang and M.G. Mason. Appl. Phys. Lett., **70** (2), 152 (1996).
39. F.J. Steemers, W.Verboom, D.N. Reihoudt, E.B. van der Tol and W. Verhoeven, J. Am. Chem. Soc., **117**, 9408 (1995).